九州大学学術情報リポジトリ
Kyushu University Institutional Repository

Preliminary Correlation Analysis of Volcano Morphology and Landslide Morphometry of the 2019 Cotabato Earthquake Series, Mindanao, Philippines

Nichole Anthony D. Pacle
Department of Geology, College of Engineering and Geosciences, Caraga State University

Karl Malcolm N. Cordova
ML-Prep Project, Mathematical and Statistical Computing Research Center, Caraga State University

Ken Adrian C. Villarias
Department of Geology, College of Engineering and Geosciences, Caraga State University

Loyd John M. Gonzales
Department of Geology, College of Engineering and Geosciences, Caraga State University

他

https://doi.org/10.5109/7395648

出版情報：Proceedings of International Exchange and Innovation Conference on Engineering & Sciences (IEICES). 11, pp.1094-1101, 2025-10-30. International Exchange and Innovation Conference on Engineering & Sciences
バージョン：
権利関係：Creative Commons Attribution-NonCommercial-NoDerivatives 4.0 International

KYUSHU UNIVERSITY

Preliminary Correlation Analysis of Volcano Morphology and Landslide Morphometry of the 2019 Cotabato Earthquake Series, Mindanao, Philippines

Nichole Anthony D. Pacle[1,*], Karl Malcolm N. Cordova[2], Ken Adrian C. Villarias[1,2], Loyd John M. Gonzales[1,2], Jay Melvin B. Segales[2], Paolo S. Pacaldo[2,3], Renz Kian A. Caballero[1], Jhon Rey A. Dela Cruz[1], Loreniel E. Anonuevo[2], Jayrold P. Arcede[2,4]
[1]Department of Geology, College of Engineering and Geosciences, Caraga State University, [2]ML-Prep Project, Mathematical and Statistical Computing Research Center, Caraga State University, [3]College of Computing and Information Sciences, Caraga State University, [4]Mathematics Department, College of Mathematics and Natural Sciences, Caraga State University
[*]Corresponding author email: ndpacle@carsu.edu.ph

Abstract: *In an earthquake-prone country such as the Philippines, earthquake geohazards such as earthquake-induced landslides (EILs) have caused widespread damage to infrastructure and communities. While studies on slope stability analysis per geologic unit already exist, these do not discriminate spatial variation within a single unit. To determine whether such variation exists–particularly within volcanic terranes, correlation analyses were performed in the Makilala-Kidapawan area of Mindanao, Philippines by using the landslide inventory of the 2019 October Cotabato earthquake series and its morphometric attributes, the volcanic morphometry and cone classes, and the geomorphological classes. Utilizing Pearson correlation analysis and ANOVA, our findings show that volcanic cones can greatly influence the surface area and morphometry of landslides as opposed to geomorphologic classes. However, the chi-squared test of volcanic cones and geomorphology show a strong association between these variables despite having a significant p-value of <0.05. The implications of this study is crucial for further investigating the dynamics of landslides on volcanic terrains.*

Keywords: Earthquake-induced landslides; Volcano morphology; Landslide morphometry, Cotabato,

1. INTRODUCTION

Between October 16 and 31, 2019, a series of high-magnitude earthquakes struck southeastern (SE) Cotabato triggered by the strike-slip movement of the Cotabato Fault System (CFS) [1]. These earthquakes, ranging from Mw 6.4 to Mw 6.8, caused widespread damage associated with earthquake-induced geohazards [2]. Earthquake-induced landslides (EILs) were recorded across SE Cotabato as documented by the Quick Response Team of the Department of Science and Technology - Philippine Institute of Volcanology and Seismology (DOST-PHIVOLCS QRT) [1]. These earthquake induced landslides are caused by the active tectonic setting of the Philippines (Fig. 1)

Slope stability assessments often simplify geotechnical parameters by generalizing them per geologic unit, using representative values [3]. While this method is effective for broad regional analyses, it falls short in explaining the varied spatial patterns of landslide morphology. This limitation is particularly evident in volcanic complexes, where diverse volcanic cone classes are often grouped as a single unit in geological maps, without distinct classification. A similar challenge arises when attempting to explain variations based on geomorphology, as a single geological unit can encompass multiple geomorphological features.

Understanding the relationship between landslide morphology and underlying volcanic and geomorphological structures is vital for enhancing localized assessments and refining landslide susceptibility models [4]. This is especially true for tectonically active regions with prominent volcanic landforms, such as Cotabato. Given that the underlying geology and associated structures influence an area's geomorphological characteristics [5], it is critical to investigate whether this influence extends to secondary hazards like EILs.

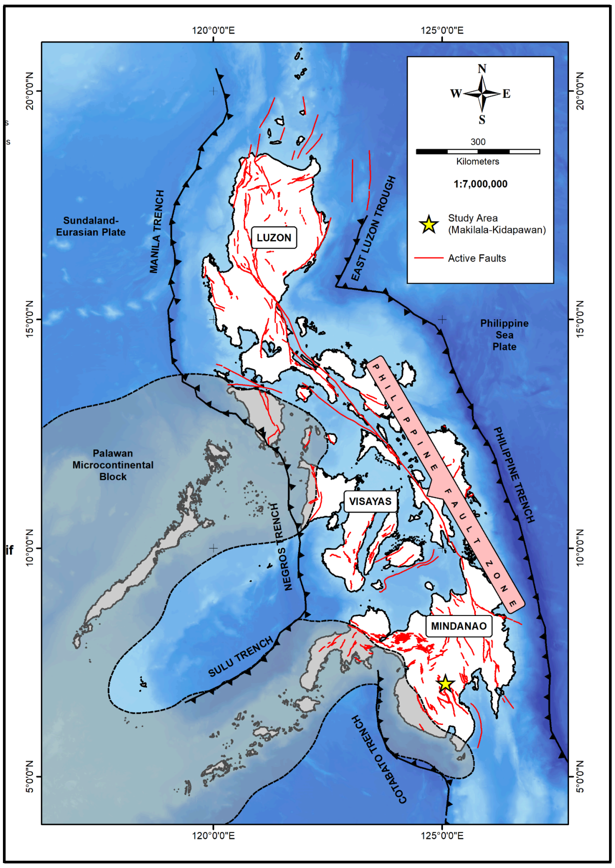

Fig. 1. Tectonic map of the Philippines modified from [6, 7]. The study area is highlighted with a star.

To address this limitation and explore potential relationships between volcanic cone types, geomorphology, and landslide morphometry in SE Cotabato, various correlation analyses are performed. The analysis integrates the: (1) landslide morphometry of the inventory of DOST-PHIVOLCS QRT [1], (2) the volcanic morphometry and classification of [8], and (3) the geomorphology classification of SE Cotabato. By investigating how variations in landslide morphology align with volcanic and geomorphological settings, this study offers a new perspective for earthquake-induced landslide hazard and risk assessments [9] in complex volcanic terrains.

1.1 Regional geology

The geologic history and tectonic evolution of the Philippines result from complex processes including rifting, oceanic spreading, subduction, and arc-continent collision [6, 10]. The Philippine archipelago, characterized as an island arc system formed through the suturing of volcanic, oceanic, and micro-continental blocks, is bordered by subduction zones on both its eastern and western flanks, contributing to widespread arc magmatism (Fig. 1) [11]. Its tectonic framework is shaped by opposing subduction systems: eastward-directed subduction along the Manila, Negros, Sulu, and Cotabato trenches in the west, and westward subduction of the Philippine Sea Plate beneath the archipelago via the Philippine and East Luzon trenches in the east [10]. The convergence of various terranes led to the development of a tectonic collage composed of distinct lithologic units, including ophiolitic complexes, metamorphic formations, magmatic arcs, and sedimentary basins [12, 13]. The current geologic framework of the Philippines is characterized by ophiolitic and metamorphic basement rocks overlain by younger volcanic sequences and substantial sedimentary basin deposits [14].

Occupying the southeastern tip of the Philippine archipelago, Mindanao stands as the country's second largest island. Its western region is defined by the Cotabato Basin and the occurrence of multiple active fault lines. The Cotabato Fault System, which plays a key role in regional seismic activity, comprises several active faults primarily arranged in two orthogonal systems: NW–SE trending Makilala-Malungon, M'lang, North and South Columbio, and Tangbulan faults, and the SW–NE trending Makilala and Balabag faults. The current strike-slip motion along these faults developed after a prior collisional event [14]. In addition to its tectonic complexity, Mindanao hosts a diverse range of volcanic features shaped by the interplay between the Eurasian and Philippine Sea plates and multiple subduction zones. Volcanic activity across the island shows a transition from arc-type magmatism older than 3 million years to more geochemically varied activity in the Quaternary, reflecting a shift in geodynamic settings [15].

2. METHODOLOGY

2.1 Materials

EIL inventory polygons were acquired from the DOST-PHIVOLCS QRT data of the 2019 Cotabato Earthquake Series. The EIL inventory consists of landslides manually delineated through remote sensing of high-resolution charter images and field validation.

A 5m Interferometric SAR digital elevation model (IfSAR DEM) from the National Mapping and Resource Information Authority (NAMRIA) dated 2013 was used as a base for generating derivative morphological data. Its finer spatial resolution provides better clarity for delineating geologic features than its moderate resolution counterparts.

Volcano morphometry data was derived from the study of [8] on the morphometric classification and distribution of volcanoes in the Philippines. For this study, only the volcano class was used. A geologic map of Makilala and Kidapawan [16, 17] was manually merged and digitized. The resulting map was further modified to encompass landforms present in the area for visual clarity. The geologic map was used to aid in the production of the geomorphological map used in the study.

2.2 Geomorphological Mapping

For generating the geomorphologic map, a method from an unpublished report by the DOST-PHIVOLCS ACER OMEGA Project [18] was used which itself was adapted from [19] for automated landform classification (Fig. 2). This novel method is a semi-automated approach for regional geomorphologic mapping using DEM and its derivative products as input for the conditional analysis of land surface parameters in a raster calculator.

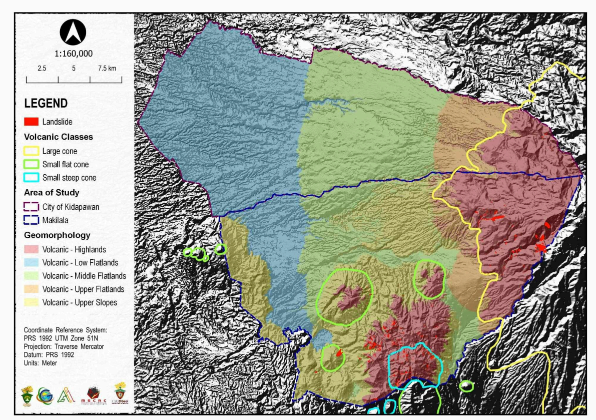

Fig. 2. Map of the study area with the identified volcanic cone classes, geomorphological classes, and the landslide inventory.

The resulting raster is reclassified and renamed according to its corresponding landform. This will further undergo post-processing to manually delineate some areas not recognized during calculation using thematic maps as reference and remove stray pixels. Finally, the landform map will be reclassified further based on its dominant lithology using the Mines and Geosciences Bureau - Regional Office No. XII (2025) geologic maps as reference [16, 17].

2.3 Landslide morphometry

Zonal statistics was used to extract landslide morphometric values. The parameters used are elevation, slope, and profile and planform curvatures. The corresponding minimum, maximum, and mean values are calculated based on the area overlain by the landslide polygons. The designation of geomorphology and volcano class is based on the majority class encompassed by the landslide polygons. There are a total of 673 landslides recorded by DOST-PHIVOLCS QRT covering SE Cotabato. For the purpose of this study, only 346 landslides were used for analysis because these correspond to the landslides intersecting with volcanic cone classes based on [8].

2.4 Correlation analysis

To establish the relationship between landslide morphometric values with geomorphology and volcanic cone classes, several correlation analyses were used and implemented in the SciPy Python library. For numerical variables corresponding to landslide morphometric values, a Pearson correlation coefficient analysis was used which creates a pairwise correlation matrix to determine the linear relationship between two landslide morphometric parameters. Moreover, the chi-squared contingency test was used to determine association between the geomorphology and volcanic classes. This test is specifically designed to analyze categorical data and determine if there is no association between them [20].

Finally, a one-way ANOVA (analysis of variance) was implemented to statistically evaluate whether geomorphology and volcanic cone classes have influence on landslide morphometric values. For every correlation analysis conducted, the corresponding p-value for every pairwise relation was evaluated for statistical significance typically <0.05.

3. RESULTS AND DISCUSSION

3.1 Distribution of landslide morphometric values versus volcano classes

In SE Cotabato, five volcanic cones classified by [8] were identified. These include one large cone which is associated with Mt. Apo volcano, three unnamed small steep cones, and one unnamed small flat cone (Fig. 2). Majority of the landslides (238 instances) were identified to have occurred within small steep cones (Fig. 3), then on large cones (80 instances), and lastly, on small flat cones (28 instances).

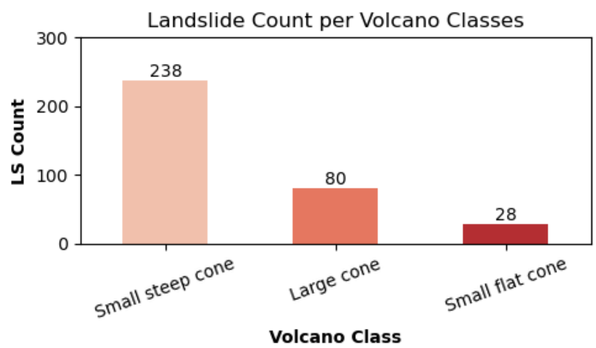

Fig. 3. Distribution of landslides per volcano class.

There are more landslides observed in areas with relatively moderate elevation which are incidentally at the same altitude as small steep cones (Fig. 4). Areas with even lower elevation like in small flat cones have fewer landslides as the slope gradually becomes stable at lower altitude. There are also fewer but larger landslides in higher elevations because of the large surface area in large cones giving the unstable slope ample space to spread out.

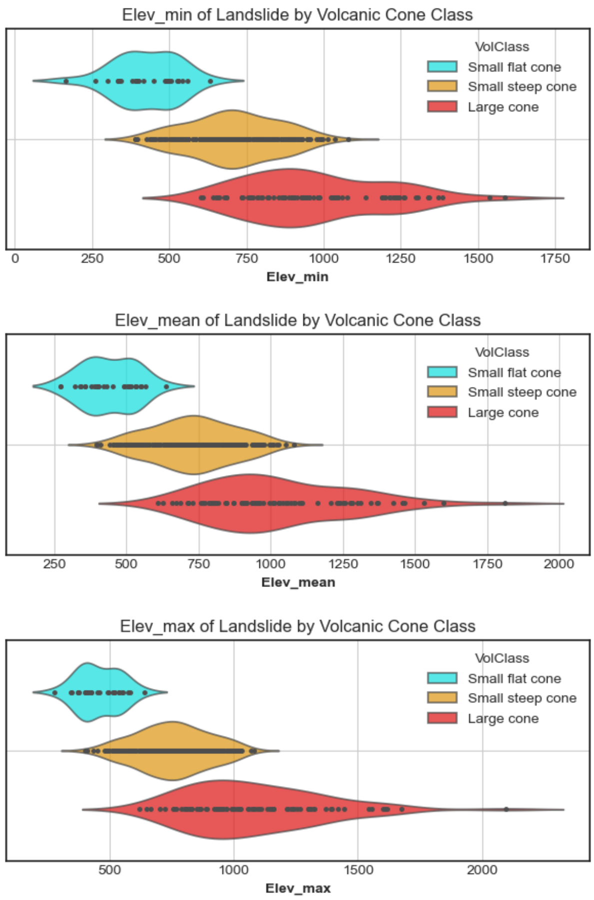

Fig. 4. Distribution of minimum, mean, and maximum landslide elevation per volcano class.

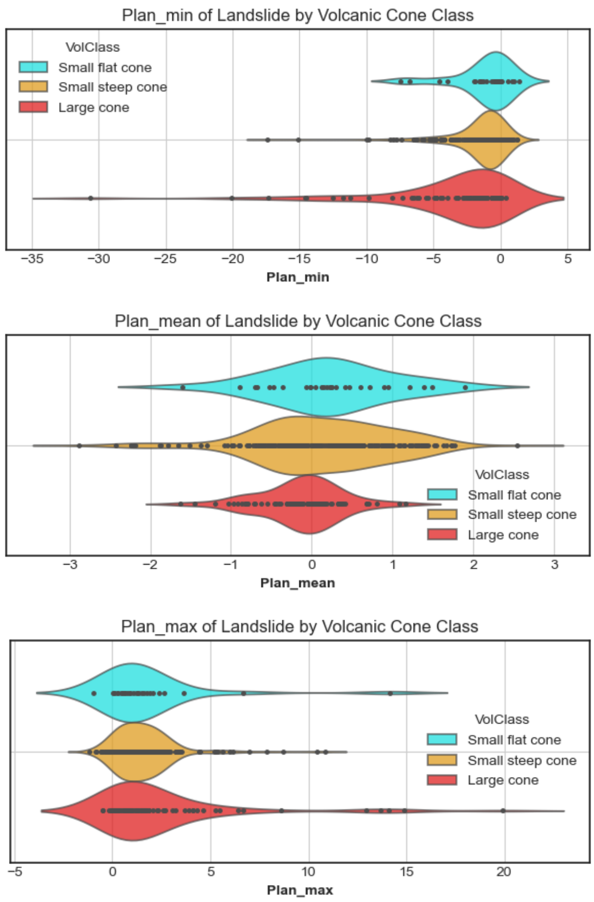

Fig. 5. Distribution of minimum, mean, and maximum landslide planar curvature per volcano class.

For the landslide morphometry attributes of the 346 landslide instances, large volcanic cones exhibit the widest range of planar curvature values (Fig. 5), suggesting that landslides here often traverse topographically complex terrain with both convergence zones and ridgelines. Meanwhile, small flat cones show planar curvature values mostly centered around zero, indicating landslides on more uniform and subdued surfaces with minimal lateral curvature. Small steep cones exhibit intermediate distributions, where curvature is slightly more variable than flat cones but less extreme than large cones, reflecting moderately dissected terrain.

Large cones again demonstrate the widest spread with regard to profile curvature (Fig. 6), with very low minimum profile curvature values (strongly concave downslope) and extremely high maximum profile curvature values (sharp convex zones), indicating high topographic relief and slope complexity within landslide areas. Small flat cones show tighter distributions across all profile curvature metrics, suggesting relatively smooth and uniform slopes with limited changes in acceleration potential. Small steep cones lie in between, with moderate variation but without the extreme curvature observed in large cones.

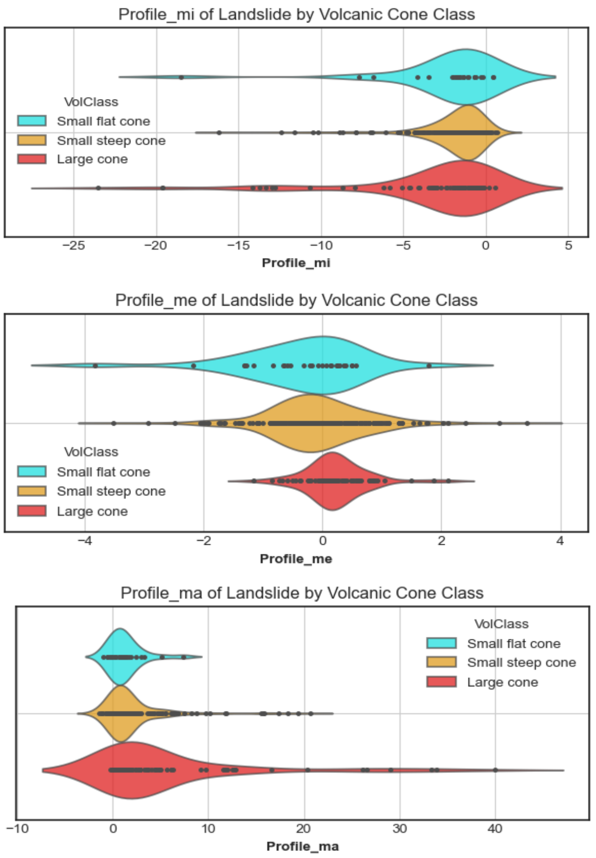

Fig. 6. Distribution of minimum, mean, and maximum landslide profile curvature per volcano class.

In terms of landslide slope angles, large cones show the widest and most variable distributions in minimum, mean, and maximum slope angles (Fig. 7). Some of these landslides extend to low slopes while still containing very steep segments, indicating complex and extensive landslides. Small steep cones exhibit consistently higher minimum slope angles, meaning landslides occur on steeper, more confined terrain. While small flat cones show generally lower mean and maximum slopes, suggesting landslides occur on gentler terrain with limited slope variability. The results correspond well to the volcanic cone classification of [8].

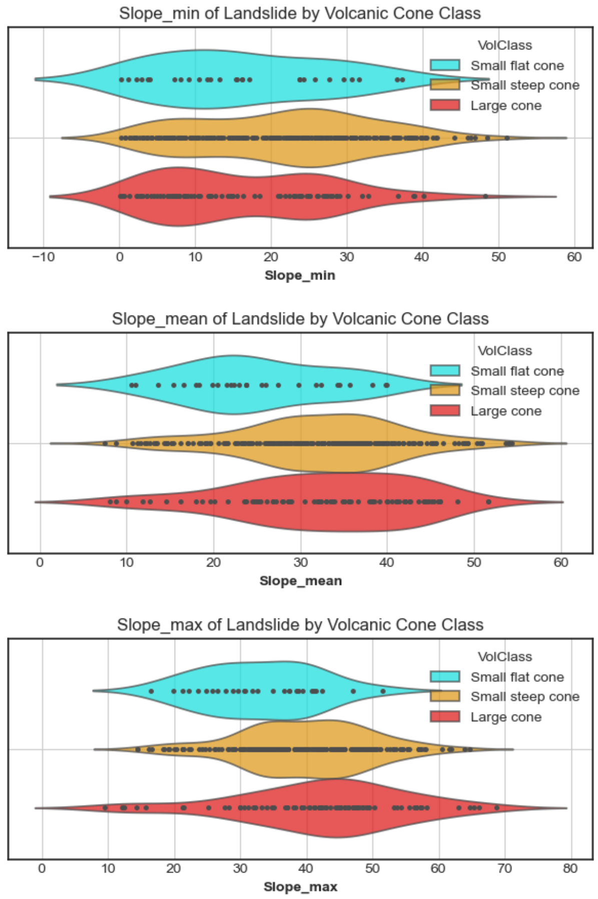

Fig. 7. Distribution of minimum, mean, and maximum landslide slope angle per volcano class.

3.2 Distribution of landslide morphometric values versus geomorphological classes

Five geomorphological units were determined but the identified landslides have only occurred on three of these units: volcanic highlands which contain the majority of the landslides (310 instances), volcanic upper slopes (33 instances), and volcanic upper flatlands (3 instances) (Fig. 8). All identified landforms were inferred as volcanic as they are proximal to Mt. Apo volcano and other unnamed volcanic cones within the study area, especially in the Makilala municipality. Majority of the landslides were identified to be part of volcanic highlands, while the remaining landslides fell under volcanic upper slopes and volcanic upper flatlands.

Landslide area of all instances in square meters (sq.m.) tends to concentrate below 50,000 sq. m. for all geomorphological classes (Figs. 8 & 9). However, volcanic upper slopes show few landslide instances with large areas, and even more prominent in volcanic highlands. In contrast, the distribution of landslide area in volcanic upper flatlands are constrained to a narrower range since there are only three instances within the class.

The distribution of landslides across all calculated morphometric attributes—planar curvature, profile curvature, and slope angle (shown in Fig. 10, 11, and 12, respectively)—reveals that landslides in volcanic highlands exhibit the widest range of values, followed by those in volcanic upper slopes. In contrast, landslides in volcanic upper flatlands show narrower ranges, primarily due to the limited number of landslide instances in this geomorphological unit.

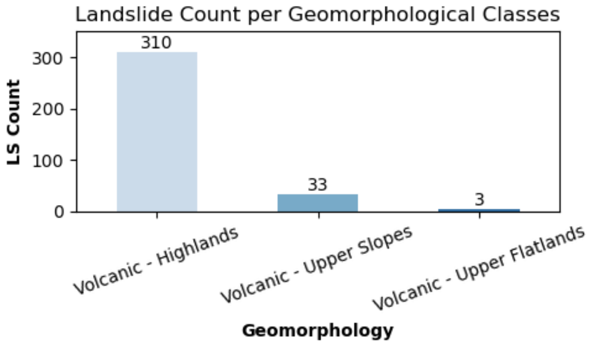

Fig. 8. Distribution of landslides per geomorphological class.

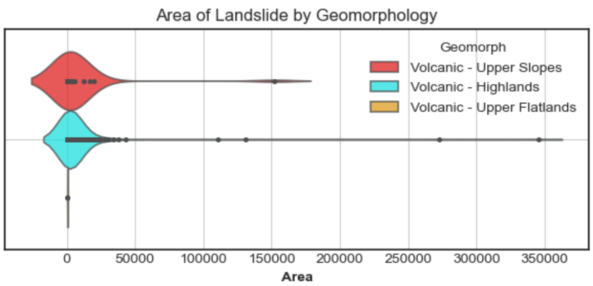

Fig. 9. Distribution of landslide area per geomorphological class.

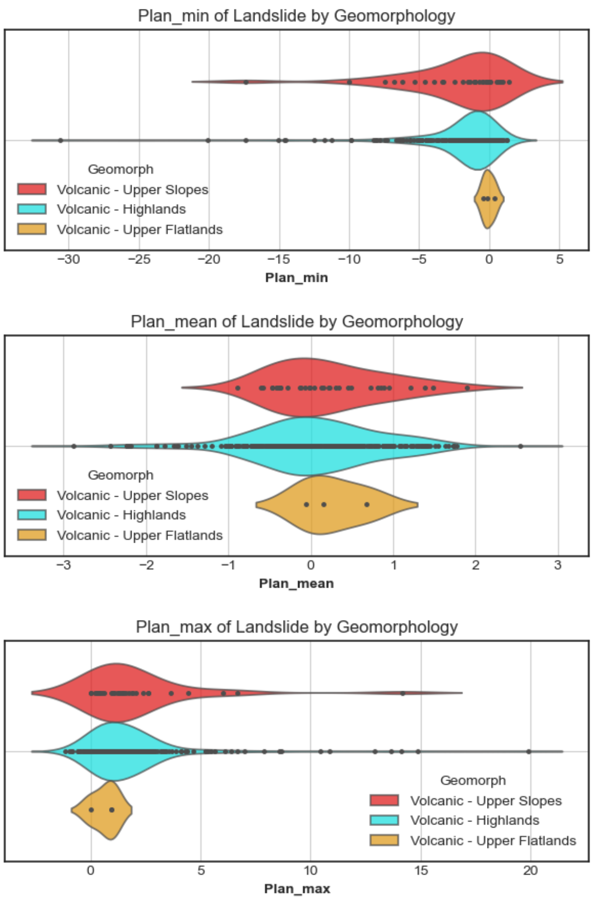

Fig. 10. Distribution of minimum, mean, and maximum planar curvature of each landslide per geomorph class.

The minimum and maximum values of planar and profile curvatures in both units (Figs. 10 & 11) exhibit broader and more variable distributions. However, their mean values remain centered around zero, suggesting that despite the wide range in curvature extremes, the average curvature within each landslide tends to balance out. As for slope angle, the minimum, mean, and maximum values also show wide variation in both volcanic highlands and volcanic upper slopes, indicating that landslides have occurred across a wide range of slope angles (Fig. 12). This suggests that no clear trend is observed between slope angle and landslide distribution in these geomorphological units.

In contrast, landslide morphometry values in volcanic upper flatlands are more concentrated, reflecting the small number of landslides observed in this unit. Nevertheless, the ranges in minimum, mean, and maximum values still reflect internal variability in morphometric attributes within each landslide instance.

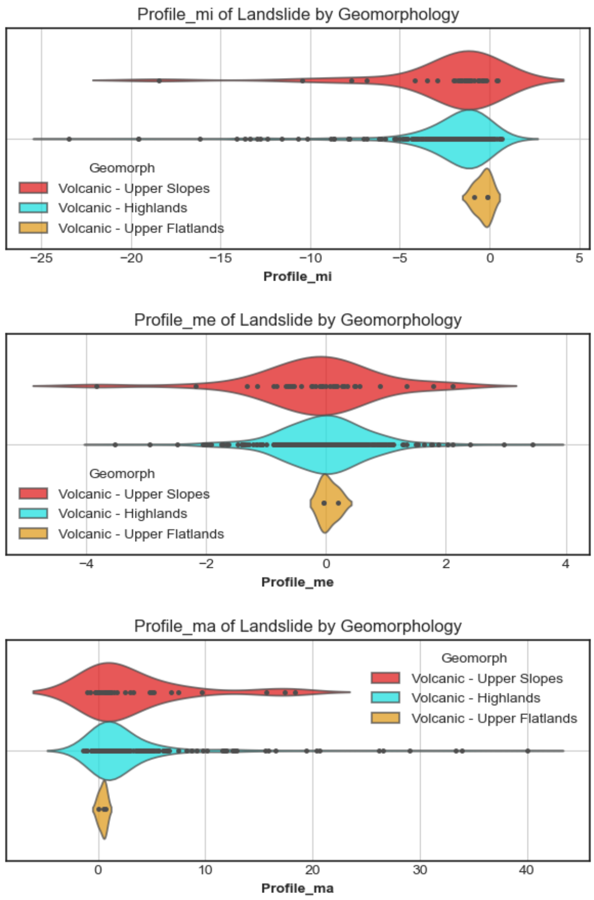

Fig. 11. Minimum, mean, and maximum profile curvature distribution of each landslide per geomorphological class.

3.3 Pearson correlation analysis of landslide morphometry values

Five initial landslide morphometry parameters (landslide surface area, elevation, slope, planform curvature, profile curvature) were used as input for Pearson correlation analysis. Of these, four parameters are derived from an IfSAR 5m DEM and calculated for their mean, minimum and maximum values bringing the total to thirteen each corresponding to their respective morphometric values.

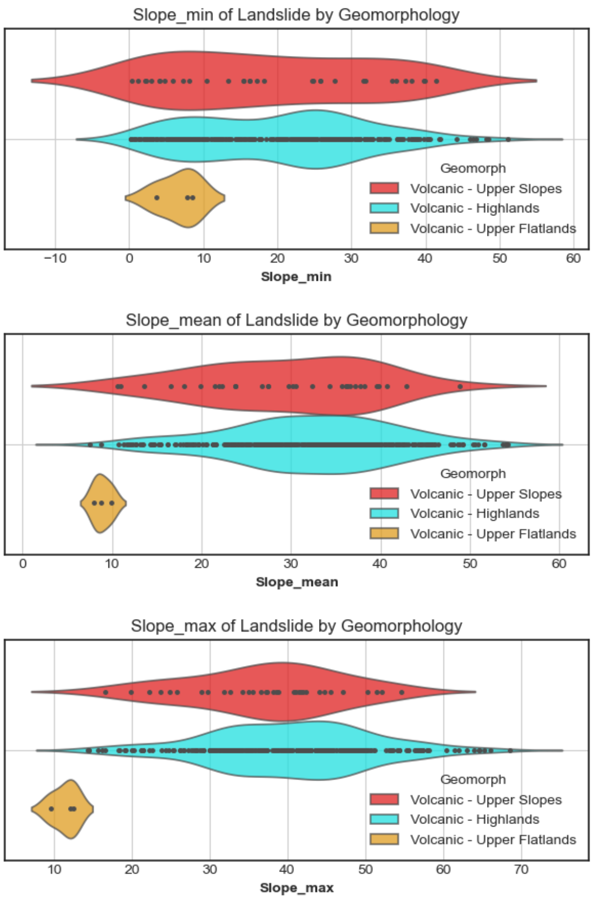

Fig. 12. Minimum, mean, and maximum slope angle distribution of each landslide per geomorphological class.

Results of the Pearson correlation analysis (Figs. 13 & 14) show that elevation and slope have very high collinearity with their respective morphometric values. Mean elevation shows high collinearity with minimum and maximum elevations as the distribution of landslides linearly increases with higher elevation. The same phenomena has been observed between the slope values.

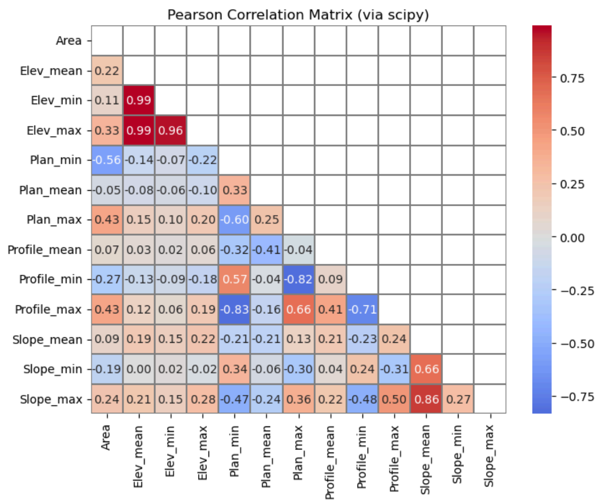

Fig. 13. Pearson correlation matrix of landslide morphometry values.

On the other hand, minimum and maximum profile and planform curvature values show an inverse relationship. Planform curvature reflects concave slopes curving outwards parallel to the steepest slope direction which is exhibited by valleys and depressions. Profile curvature reflects convex terrains curving inwards perpendicular to the maximum slope typical in ridges and mountaintops. An increase in either curvature value will decrease the value of its counterpart. The rest of the morphometric values show weak to no correlation indicating independence among the parameters used.

The p-value was calculated from the resulting correlation coefficients to assess their statistical significance (<0.05). Minimum slope and mean elevation showed the lowest statistical significance followed by mean profile and minimum elevation (Fig. 14). While some variables do not exhibit statistical significance, the results of both the Pearson correlation and p-value calculation shows that there is generally no linear relationship among variables. Additionally, variables which exhibit pairwise dependence due to their high correlation coefficient show statistical significance having a p-value of <0.05. Because of this, no variables were dropped in subsequent analysis.

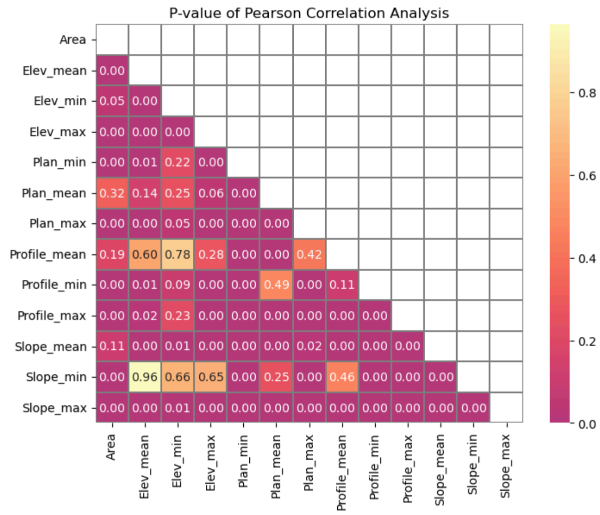

Fig. 14. P-value of the Pearson correlation coefficients of landslide morphometric values.

3.4 Chi-squared test

A chi-squared test is conducted to test the independence of geomorphology and volcano classes (Table 1). The large chi-squared value in comparison to the expected frequencies of geomorphology and volcano classes show that these variables have a strong association with each other. A p-value of <0.05 shows that this result is statistically significant despite low observed frequencies in the upper flatlands. This is because there are fewer landslides observed in the upper flatlands than in any other geomorphology.

Table 1. Chi-squared test results

Chi-squared statistic: 118.13
Degrees of freedom: 4
P-value: 1.34e-24

	Large cone	*Small flat cone*	*Small steep cone*
Highlands	71.67	25.09	213. 24
Upper Flatlands	0.69	0.24	2.06
Upper Slopes	7.63	2.67	22.7

3.5 ANOVA Results

A one-way ANOVA (analysis of variance) was conducted to assess how geomorphology and volcanic cone classes influence landslide morphometry values. A forest plot showing the effect size (η^2) was also used to visualize the strength of the relationship of each landslide morphometric parameters with geomorphology and volcanic cone classes at a 95% confidence interval. Effect sizes were interpreted based on established thresholds [20]where $\eta^2 \geq 0.01$ indicating small effect, $\eta^2 \geq 0.06$ indicating medium effect, and $\eta^2 \geq 0.14$ indicating large effect size.

The results of one-way ANOVA of geomorphology and landslide morphometry values show that only five morphometric values are statistically significant having a p-value of <0.05 (Fig. 15 and Table 2). The forest plot of the eta-squared (η^2) effect size metrics also show that only elevation values have the largest effect size while slope values have an effect size ranging from small to medium. The results suggest that there is a poor relationship between geomorphology and landslide morphometric values. As such, geomorphology cannot necessarily influence landslide morphometric values.

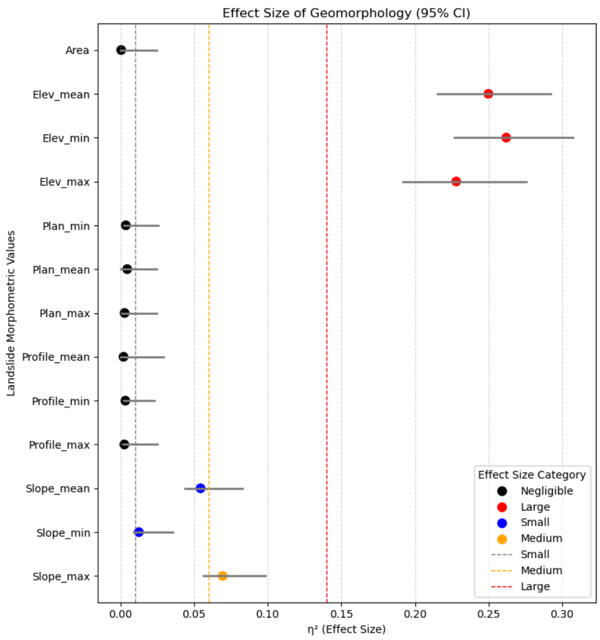

Fig. 15. Forest plot illustrating the effect size of landslide morphometric values with geomorphology.

Table 2. One-way ANOVA results of geomorphology

Variable	F-statistics	P-value
Area	0.098	0.907
Elev_mean	57.147	0.000
Elev_min	60.903	0.000
Elev_max	50.673	0.000
Plan_min	0.641	0.5273
Plan_mean	0.798	0.4509
Plan_max	0.494	0.6105
Profile_mean	0.366	0.6937
Profile_min	0.581	0.5597
Profile_max	0.464	0.6294
Slope_mean	9.877	0.0001
Slope_min	2.183	0.1142
Slope_max	12.809	0.000

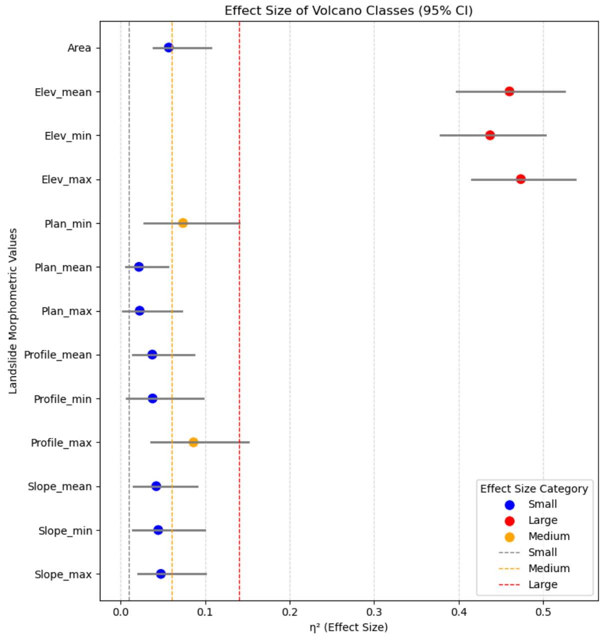

Fig. 16. Forest plot illustrating the effect size of landslide morphometric values with volcanic cones.

For the results of ANOVA with volcanic cone classes, all parameters show a high statistical significance with p-value<0.05 which indicates that volcanic cones are associated with and may influence landslide morphometric values (Fig. 16 & Table 3). Forest plots of the volcanic cone classes also show that elevation values have the largest effect followed by minimum planform curvature and maximum profile curvature. The rest of the parameters have small effect size with volcano classes. This implies that elevation values have a strong relationship with both geomorphology and volcanic cones as most landslides were found in areas with high elevation.

Table 3. One-way ANOVA results of volcanic cones

Variable	F-statistics	P-value
Area	10.355	0.000
Elev_mean	146.216	0.000
Elev_min	133.281	0.000
Elev_max	154.356	0.000
Plan_min	13.67	0.000
Plan_mean	3.798	0.0234
Plan_max	3.951	0.0201
Profile_mean	6.678	0.0014
Profile_min	6.747	0.0013
Profile_max	16.19	0.000
Slope_mean	7.542	0.0006
Slope_min	7.985	0.0004
Slope_max	8.578	0.0002

4. CONCLUSIONS AND RECOMMENDATIONS

The study demonstrates that volcanic cone classes significantly influence the morphometric characteristics of earthquake-induced landslides in SE Cotabato. Statistical analyses, particularly ANOVA, revealed strong correlations between volcanic morphology and landslide morphometric attributes such as elevation, slope, and curvature. Landslides on large volcanic cones tend to exhibit more complex terrain features and wider morphometric ranges. In contrast, geomorphological classes showed weaker relationships with landslide attributes, indicating limited insight towards the resulting landslide morphometry. These findings suggest that volcanic morphology is a more effective parameter for assessing landslide susceptibility in volcanic terrains.

Given the strong influence of volcanic cone classes on the landslide morphometric values, a more detailed volcanic landform subclassification or volcano geologic map is recommended. The significant impacts of the volcano morphology to the landslide morphometry can also elucidate the linkage of the physical and chemical properties of the soil and bedrock within these EILs. It also allows for more targeted mitigation strategies as well as more refined EIL predictions in specific volcanic terrains.

5. REFERENCES

[1] J. S. Perez, D. J. Buhay, *et al.*, "Fault geometry and geologic impacts of the 15 December 2019 Magnitude 6.9 Davao del Sur Earthquake," *Geol. Conv. 2020*, 2019, doi: 10.5281/zenodo.10885398

[2] M. F. Ferrario, J. S. Perez, M. Dizon, F. Livio, J. Rimando, and A. M. Michetti, "Environmental effects following a seismic sequence: the 2019 Cotabato—Davao del Sur (Philippines) earthquakes," *Nat. Hazards*, vol. 120, pp. 6125–6147, 2024, doi: 10.1007/s11069-024-06467-7

[3] R. W. Jibson, E. L. Harp, and J. A. Michael, "A method for producing digital probabilistic seismic landslide hazard maps," *Eng. Geol.*, vol. 58, pp. 271–289, 2000, doi: 10.1016/S0013-7952(00)00039-9.

[4] S. Vingiani, G. Mele, R. De Mascellis, F. Terribile, and A. Basile, "Volcanic soils and landslides: A case study of the island of Ischia (southern Italy) and its relationship with other Campania events," *Solid Earth*, vol. 6, no. 2, pp. 783–797, 2015, doi: 10.5194/se-6-783-2015.

[5] K. P. Arreza, J. E. Tidoy, S. A. Salcedo-Albores, P. S. Buenavista, and N.A.D. Pacle, "Investigating the Impact of Lithology and Lineament Structures to the Drainage Morphometry of Carrascal Watershed, Surigao Del Sur, Mindanao, Philippines Using Correlation and Principal Component Analyses," *Proceedings of International Exchange and Innovation Conference on Engineering & Sciences (IEICES)*. 10, pp.1198-1204, 2024-10-17. https://doi.org/10.5109/7323409

[6] M. A. Aurelio, R. E. Peña, and K. J. L. Taguibao, "Sculpting the Philippine archipelago since the Cretaceous through rifting, oceanic spreading, subduction, obduction, collision and strike-slip faulting: Contribution to IGMA5000," *J. Asian Earth Sci.*, vol. 72, pp. 102–107, 2013.

[7] N.A.D. Pacle, C. B. Dimalanta, N. T. Ramos, B.D. Payot, D. V. Faustino-Eslava, K. L. Queaño, and G. P. Yumul Jr., "Petrography and geochemistry of Cenozoic sedimentary sequences of the southern Samar Island, Philippines: Clues to the unroofing history of an ancient subduction zone". J. of Asian Earth Sci. 2017.

[8] E. M. Paguican, P. Grosse, G. N. Fabbro, and M. Kervyn, "Morphometric classification and spatial distribution of Philippine volcanoes," *J. Volcanol. Geotherm. Res.*, vol. 418, p. 107251, 2021, doi: 10.1016/j.jvolgeores.2021.107251.

[9] S. Maryanto, M. A. Widyaminudiin, D. A. Suaidi, C. A. Perwita, S. D. Wuryani, S. Abe, A. Yoshikawa, E. M. H. Takla, K. M. Girgis, R. P. H. Sari, and V. Syahra, "Multi-method geophysical observations in governing sustainable development of a volcano-hosted geothermal area in Cangar, Indonesia," *Proceedings of International Exchange and Innovation Conference on Engineering & Sciences (IEICES)*. 10, pp. 1205–1211, 2024-10-17. https://doi.org/10.5109/7323410

[10] C. B. Dimalanta, R. C. Salapare, D. V. Faustino-Eslava, N. T. Ramos, K. L. Queaño, G. P. Yumul Jr., and T. F. Yang, "Post-emplacement history of the Zambales Ophiolite Complex: Insights from petrography, geochronology and geochemistry of Neogene clastic rocks," *J. Asian Earth Sci.*, vol. 104, pp. 215–227, 2015.

[11] G. P. Yumul Jr., C. B. Dimalanta, E. J. Marquez, and K. L. Queaño, "Onland signatures of the Palawan microcontinental block and Philippine mobile belt collision and crustal growth process: A review," *J. Asian Earth Sci.*, vol. 34, no. 5, pp. 610–623, 2009.

[12] M. A. Aurelio, "Shear partitioning in the Philippines: Constraints from Philippine Fault and global positioning system data," *Island Arc*, vol. 9, no. 4, pp. 584–597, 2000.

[13] M. A. A. Casulla, H. Mizunaga, T. Tanaka, and C. Dimalanta, "Understanding the Geology of the Philippines through Gravity Anomalies," *J. Asian Earth Sci.*, 2021.

[14] R. D. Quebral, M. Pubellier, and C. Rangin, "The onset of movement on the Philippine Fault in eastern Mindanao: A transition from a collision to a strike‐slip environment," *Tectonics*, vol. 15, no. 4, pp. 713–726, 1996.

[15] F. G. Sajona, H. Bellon, R. Maury, M. Pubellier, J. Cotten, and C. Rangin, "Magmatic response to abrupt changes in geodynamic settings: Pliocene—Quaternary calc-alkaline and Nb-enriched lavas from Mindanao (Philippines)," *Tectonophysics*, vol. 237, no. 1–2, pp. 47–72, 1994, doi: 10.1016/0040-1951(94)90158-9.

[16] Mines and Geosciences Bureau – Regional Office No. XII, *Geologic map of Municipality of Makilala*, 1:175,000 scale, 2025.

[17] Mines and Geosciences Bureau – Regional Office No. XII, *Geologic map of Kidapawan City*, 2025.

[18] ACER Program - OMEGA Project, *Regional Geomorphic Mapping*, unpublished manuscript, Philippine Institute of Volcanology and Seismology, 2024.

[19] A. Weiss, "Topographic position and landforms analysis," Poster presented at *ESRI User Conference*, San Diego, CA, vol. 64, pp. 227–245, 2001. [Online]. https://www.jennessent.com/downloads/TPI-poster-TNC_18x22.pdf

[20] R. Rana and R. Singhal, "Chi-square test and its application in hypothesis testing," *J. Pract. Cardiovasc. Sci.*, vol. 1, no. 1, pp. 69–71, Jan.–Apr. 2015, doi: 10.4103/2395-5414.15757

[21] J. Cohen, *Statistical Power Analysis for the Behavioral Sciences*, 2nd ed. New York, NY, USA: Routledge, 1988. doi: 10.4324/9780203771587.